GASTROINTESTINAL

CrossMark

Virtual monoenergetic dual-layer, dual-energy CT enterography: optimization of keV settings and its added value for Crohn's disease

Sang Min Lee[1] · Se Hyung Kim[2,3] · Su Joa Ahn[2,3] · Hyo-Jin Kang[2,3] · Ji Hee Kang[2] · Joon Koo Han[2,3,4]

Abstract

Objectives To determine the optimal keV on dual-layer, dual-energy CT enterography (dlDE-CTE) and to investigate the added value of virtual monoenergetic images (VMIs) for the diagnosis of active Crohn's disease (CD).

Methods We collected 76 patients (including 45 CD patients) who underwent dlDE-CTE. CD was diagnosed using ileocolonoscopy. Conventional polychromatic images (PCI) were reconstructed using an iterative reconstruction algorithm at 120 kVp, and VMI at 40 keV (VMI_{40}), 55 keV (VMI_{55}), and 70 keV (VMI_{70}). Contrast-to-noise ratio (CNR) was compared using Kruskal-Wallis test. Three radiologists independently reviewed PCI and subsequently combined PCI and the optimized VMI for the diagnosis of active CD using a 5-point scale. Multi-reader multi-case receiver operating characteristic analysis was performed.

Results Mean ± standard deviation of CNRs for both normal (13.6 ± 6.5, 6.1 ± 3.2, 2.0 ± 2.1, 1.9 ± 1.6; $P<0.001$) and abnormal (9.4 ± 7.3, 6.5 ± 4.8, 4.9 ± 3.1, 3.7 ± 2.3; $P<0.001$) bowels were significantly greatest on VMI_{40}, followed by VMI_{55}, VMI_{70}, and PCI. When VMI_{40} were added to PCI, overall area-under-the-curve of the three radiologists was significantly improved from 0.891 to 0.951 for diagnosing active CD ($P=0.009$).

Conclusions The lowest monoenergetic images (VMI_{40}) provided the best CNR on dlDE-CTE. Furthermore, the diagnostic performance for diagnosing active CD can be significantly improved with the addition of VMI_{40}.

Key Points

• *CNR for both normal and abnormal bowel walls is greatest on VMI_{40}.*

• *Subjective image quality on VMI_{40} is better than those on PCI.*

• *When VMI_{40} images are added to PCI, radiologists' diagnostic performance can be improved.*

Keywords Small bowel · Crohn's disease · Diagnostic performance · Dual-energy CT enterography · Spectral CT

Abbreviations

MDCT	Multidetector CT
CTE	CT enterography
DE	Dual energy
SDCT	Spectral detector CT
dlDE-CTE	Dual-layer dual-energy CTE
PCI	Polychromatic image
VMI	Virtual monoenergetic image
CNR	Contrast-to-noise ratio
ROC	Receiver operating characteristic
AUC	Area under the curve
ANOVA	One-way analysis of variance
SD	Standard deviation

✉ Se Hyung Kim
shkim7071@gmail.com

1 Department of Radiology, Hallym University Sacred Heart Hospital, Anyang, South Korea

2 Department of Radiology, Seoul National University Hospital, 101 Daehangno, Jongno-gu, Seoul 03080, Korea

3 Department of Radiology, Seoul National University College of Medicine, 101 Daehangno, Jongno-gu, Seoul 03080, Korea

4 Institute of Radiation Medicine, Seoul National University Medical Research Center, Seoul, South Korea

Introduction

By virtue of the introduction of multi-detector row CT (MDCT), as well as new oral contrast agents, CT enterography (CTE) has become one of the primary diagnostic modalities for the evaluation and management of suspected or known small bowel diseases [1–4]. Until now, various elaborate CT parameters for CTE have been established to maximize the visualization of enhancing bowel loops and small bowel tumours [5, 6]. However, according to recent meta-analysis

Springer

studies [7, 8], the diagnostic performance of CTE for the diagnosis of small bowel diseases has shown wide variability in both sensitivity and specificity, in which CTE provided 74~92% sensitivity and 11~97% specificity for the diagnosis of small bowel Crohn's disease. This wide range in diagnostic performance may be partially due to the inhomogeneous study groups. As an example, if many patients with early stage Crohn's disease were included in a certain study, diagnostic accuracy may decrease as Crohn's disease may manifest only as subtle mucosal enhancement in its early stage on CTE [9]. Therefore, to enhance the diagnostic accuracy even in the early stages of Crohn's disease, lower kVp images may be used as low kVp can maximize the contrast from intravenous contrast agents. Yet, lowering the kVp below a certain threshold will eventually result in unacceptable deterioration of diagnostic performance primarily owing to the correlative increase in image noise [10]. Thus, to circumvent this limitation, several techniques including virtual monoenergetic images (VMI) from dual-energy acquisition and iterative reconstruction have been developed [11, 12].

Conventional polychromatic CT scanning is accomplished using a single source polychromatic X-ray beam in which the upper limit of the energy spectrum (or peak energy) is manually chosen. To the contrary, VMI uses a complex post-processing algorithm on dual-energy data sets to produce computed images at a single chosen "monoenergetic" energy level. Reconstructions at high keV reduce beam hardening artefacts while reconstructions at low keV maximizes the contrast from intravenous contrast agents as they more closely approximate the k edge of iodine (33 keV), and these VMI images can be produced using CT images if both high and low energy CT are obtained. Unlike with other dual-energy CT (DECT) techniques such as dual-source DECT or rapid-switching DECT [13], because dual-layer dual-energy CT (dlDECT) requires no pre-scan determination, there is no need to call the patients back for additional spectral analysis. In addition, on-demand spectral analysis of a region of interest allows the physician to further investigate incidental findings. The approach to this spectral CT is based on a unique detector design built of two scintillating layers, in which the upper layer mostly captures the low energy X-ray photons while the lower layer mostly captures the high energy photons. With this design, every scan can provide spectral information.

However, even though the effect of VMI and optimal energy reconstruction levels in small bowel obstruction has been recently reported [11], its utility for other small bowel diseases has not yet been reported. Furthermore, the previous investigation used dual-source, dual-energy CT which is different from the SDCT used in our study. Therefore, the purpose of our study is to find the optimal monoenergetic keV setting for

maximum contrast-to-noise (CNR) on dual-layer dual-energy CTE (dlDE-CTE), and to investigate the added value of VMI for the detection of active Crohn's disease.

Materials and methods

Study population

This retrospective study was approved by the ethics committee of our institution (Seoul National University Hospital, Seoul, Korea) and the requirement for informed consent was waived. Between June 2016 and April 2017, 112 consecutive patients who underwent dlDE-CTE (IQon Spectral CT, Philips Healthcare, Cleveland, OH, USA) due to suspected small bowel disease were enrolled. Eligibility criteria were as follows: (a) patients older than 18 years old, (b) patients who underwent dlDE-CTE with available reconstruction of monoenergetic spectral reconstruction images, (c) patients with available clinical data including endoscopic, histopathologic, or clinical findings and (d) patients with no contraindication to iodine contrast media due to renal failure (glomerular filtration rate, GFR < 30mL/min) or previous adverse reaction to iodine contrast media. The electric medical records regarding endoscopic findings, pathologic findings, laboratory finding, past medical history, medication, operation history, and clinical course and dlDE-CTE images were reviewed by two radiologists (S.H.K. and S.M.L., more than 15 years and 9 years of experience in abdominal imaging, respectively) in consensus.

In total, 36 patients who had alternative diagnosis other than active Crohn's disease (n=15) and had no available clinical or pathological data (n=21) were excluded. Of the remaining patients, 45 patients were diagnosed as having active Crohn's disease by means of ileocolonoscopy with or without endoscopic biopsy. The remaining 31 patients were confirmed as normal with no specific bowel disease and no symptoms on close follow-up. Finally, 76 patients (38 men and 38 women; mean age ± standard deviation, 41.5 ± 15.0 years) consisting of 45 patients (27 men and 18 women; mean age ± standard deviation, 35.8 ± 12.7 years) with active Crohn's disease (disease group) and 31 patients (11 men and 20 women; mean age ± standard deviation, 49.8 ± 14.4 years) without small bowel disease (control group) were enrolled in our study (Fig. 1). The median interval between dlDE-CTE and recent ileocolonoscopy was 14 days (range, 0-27 days). The median follow-up period for the control group was 63 days (range, 7-135 days).

dlDE-CTE acquisition and image reconstruction

All patients were asked to intake 1350 mL of a low-Hounsfield unit enteric contrast agent (Easymark, Taejoon
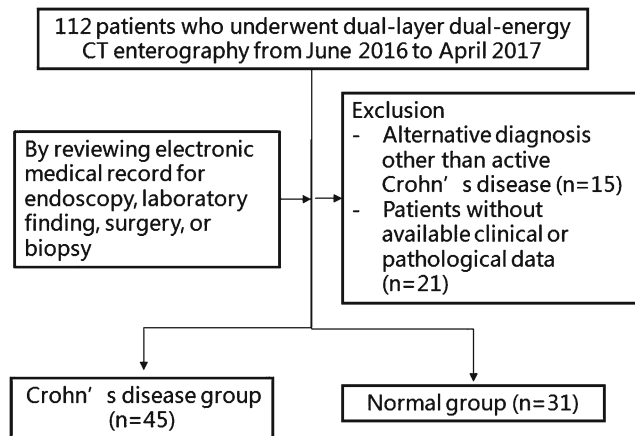
Fig. 1. Flow diagram of the study population.

Table 1. Comparative results of qualitative analysis between PCI-iDose[4] and VMI40

	PCI-iDose[4]	VMI40	P Values*
Contrast	3.3 ± 0.6	4.3 ± 0.6	**<0.001**
Image noise	4.0 ± 0.5	3.5 ± 0.6	**<0.001**
Overall image quality	3.8 ± 0.6	3.9 ± 0.7	0.059

Data are mean ± standard deviation. *P values were calculated using the Wilcoxon signed rank test. P values in **Bold Italics** represent statistical significance. PCI-iDose[4] =conventional polychromatic images obtained at 120 kVp reconstructed using iterative reconstruction (iDose[4]), VMI40=virtual monoenergetic images reconstructed at 40 keV on dual-layer dual-energy CT.

Pharmaceuticals, Seoul, Korea) during 1 h prior to CT scanning. All dlDE-CTE examinations were performed using dual-layer, dual-energy CT (IQon Spectral CT, Philips Healthcare, Cleveland, OH, USA) with tube voltages of 120 kVp. Automated tube current modulation was applied. An intravenous contrast agent (iohexol; Bonorex 350, Central Medical Service, Seoul, South Korea) with a total amount of 1.6 mL/kg of body weight was administered at a rate of 3-5 mL/s for the fixed 30 s using a power injector system. CT images were obtained at enteric and portal phases. For the enteric phase, a 35 s delay was used after the aorta reached 100 HU using the bolus tracking method. For the portal phase, a fixed 70 s delay was used after contrast administration.

For enteric phase images, conventional polychromatic images were reconstructed at 120 kVp using an iterative reconstruction algorithm, iDose[4] (PCI-iDose[4]). Virtual monoenergetic images were also reconstructed at 40 keV (VMI40), 55 keV (VMI55), and 70 keV (VMI70). For VMI, iterative reconstruction algorithm, iDose[4] level 4 was also

used. 55 keV and 70 keV were selected because 55 keV monoenergetic images are equivalent to 80 kVp (low kVp) images and 70 keV monoenergetic images are equivalent to 120 kVp (standard kVp) images. The rationale to select 40 keV images was because 40 keV is the lowest keV setting provided by the software. All conventional and VMI images were reconstructed on both axial and coronal planes with 3 mm slice thickness and 2 mm reconstruction interval. Only enteric phase images were used for further image analysis.

To analyse the radiation exposure of sDE-CTE, the CT dose index volume ($CTDI_{vol}$) and dose length product (DLP) were recorded for each CT examination. The effective radiation dose was calculated by multiplying the DLP by a conversion factor (0.015 mSv/mGy·cm) [14].

Quantitative image analysis

For each reconstructed image (PCI-iDose[4], VMI40, VMI55, and VMI70) of all patients, the contrast-to-noise ratio (CNR_N) for the normal bowel wall were calculated by one

Fig. 2. Comparative results of contrast-to-noise ratios (CNRs) in normal and abnormal bowel walls. CNR for both normal (CNR_N) and abnormal bowel walls (CNR_{AB}) was greatest on VMI55, followed by VMI55, VMI70, and PCI-iDose[4]. Post hoc test revealed that all comparisons except CNR_N between PCI-iDose[4] and VMI70 were statistically significant. PCI-iDose[4] represents the conventional polychromatic image obtained at 120 kVp reconstructed using iterative reconstruction (iDose[4]) and VMI40-70 indicates virtual monoenergetic images reconstructed at 40-70 keV on dual-layer, dual-energy CT.
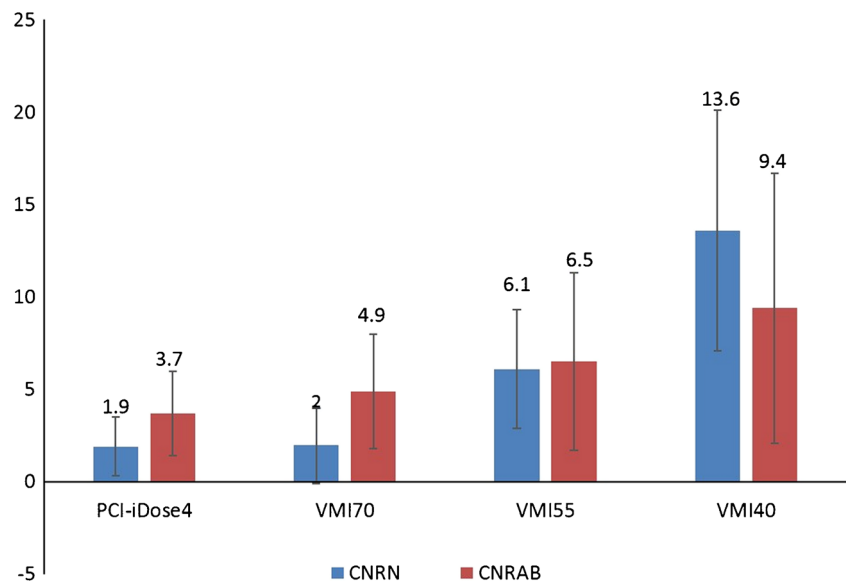
Table 2. Comparison of AUC as diagnostic performance for active Crohn's disease

Radiologist	PCI-iDose[4]	PCI-iDose[4] + VMI$_{40}$	Difference	P Values
1	0.875 (0.779,0.940)	0.943 (0.864,0.983)	-0.077 (-0.144-0.009)	*0.027*
2	0.882 (0.788,0.945)	0.959 (0.887,0.991)	-0.067 (-0.127-0.008)	*0.027*
3	0.915 (0.829,0.967)	0.952 (0.877,0.988)	-0.037 (-0.070-0.003)	*0.035*
Overall	0.891 (0.842,0.940)	0.951 (0.918,0.984)	-0.060 (-0.099-0.021)	*0.009**

Numbers in parentheses are 95% confidence interval.

* *P* values were calculated using a multi-reader, multi-case receiver operating characteristic (MRMC ROC) analysis. AUC= area under the ROC curve, PCI-iDose[4] =conventional polychromatic images obtained at 120 kVp reconstructed using iterative reconstruction (iDose[4]), VMI$_{40}$=virtual monoenergetic images reconstructed at 40 keV on dual-layer dual-energy CT.

radiologist (S.M.L.). In the 45 cases with active Crohn's disease, CNR$_{AB}$ for the abnormal bowel wall was also measured. Abnormal bowel wall was defined when mural hyperenhancement (increased enhancement compared to adjacent normal small bowel loops) [15, 16] or mural thickening ($\geq$ 3 mm) [7] and determined by two radiologists (S.H.K. and S.M.L.) in consensus. For abnormal bowel wall, ROI was placed on only the enhancing portion of the diseased bowel.

The CNR of normal bowel walls were derived using the following formula: $CNR_N = \{[(AV_{N1}+AV_{N2})/2]-AV_{GM}\}/SD_{GM}$, where AV_N is the attenuation value of the normal bowel wall, GM represents the gluteal muscle, and SD is the abbreviation for standard deviation. The CNR of abnormal bowel walls was derived using the following equation: $CNR_{AB} = (AV_{AB}-AV_N)/[(SD_{AB}+SD_N)/2]$, where AV is the attenuation value, AB is the abnormal bowel wall, N is the normal bowel wall, and SD is the standard deviation [11, 17].

For these parameters, regions of interest (ROIs) were carefully placed by one radiologist (S.M.L) so as to avoid artefacts. To place ROIs of the same size and shape at the same location in each reconstructed image, the "copy and paste" function was applied on picture archiving and communication system (PACS) monitors. The mean size of ROIs for the normal or abnormal bowel wall, and gluteus muscle was 9.4 mm^2, 17.0 mm^2, and 63.6 mm^2, respectively.

Qualitative image analysis

For PCI-iDose[4] and VMI at the keV setting optimized via quantitative analysis, subjective image quality was also assessed by different three radiologists of various expertise (J.H.K., H.J.K., and S.J.A. with experience in abdominal imaging of 2, 5, and 7 years, respectively) who were blinded to the final diagnosis. They graded the images in terms of contrast, noise, and overall image quality using a 5-point scale [18]. Contrast was graded as follows: 1, images similar to the use of no contrast, non-diagnostic; 2, poor contrast and unsatisfactory visualization; 3, good contrast; 4, very good contrast; and 5, excellent contrast. Noise was graded as: 1, high level noise, non-diagnostic; 2, significant noise affecting diagnosis; 3, noisy but diagnostic; 4, no significant noise; and 5, minimal or absent noise. Overall image quality was graded as follows: 1, diagnostically unacceptable; 2, suboptimal for diagnosis; 3, average; 4, better than average; and 5, excellent.

Diagnostic performances

To assess the improvement of radiologists' diagnostic performance with the addition of optimized VMI (i.e., VMI$_{40}$), two successive review sessions for the diagnosis of active Crohn's disease were independently performed by the three radiologists. At the first session, radiologists interpreted only conventional polychromatic CTE images reconstructed with iDose[4]

Table 3. Diagnostic Accuracy for Active Crohn's disease

Radiologist	PCI-iDose[4]				PCI-iDose[4] + VMI$_{40}$			
	Sensitivity	Specificity	PPV	NPV	Sensitivity	Specificity	PPV	NPV
1	66.7%	90.3%	90.9%	65.1%	95.6%	93.6%	95.6%	93.6%
2	82.2%	90.3%	92.5%	77.8%	93.3%	93.6%	95.5%	90.6%
3	86.7%	90.3%	82.9%	82.4%	97.8%	96.3%	97.8%	96.3%
Overall	78.5%	90.3%	92.2%	74.3%	95.6%	90.3%	93.5%	93.3%

PCI-iDose[4] =conventional polychromatic images obtained at 120 kVp reconstructed using iterative reconstruction (iDose[4]), VMI$_{40}$=virtual monoenergetic images reconstructed at 40 keV on dual-layer dual-energy CT, PPV= positive predictive value, NPV= negative predictive value.
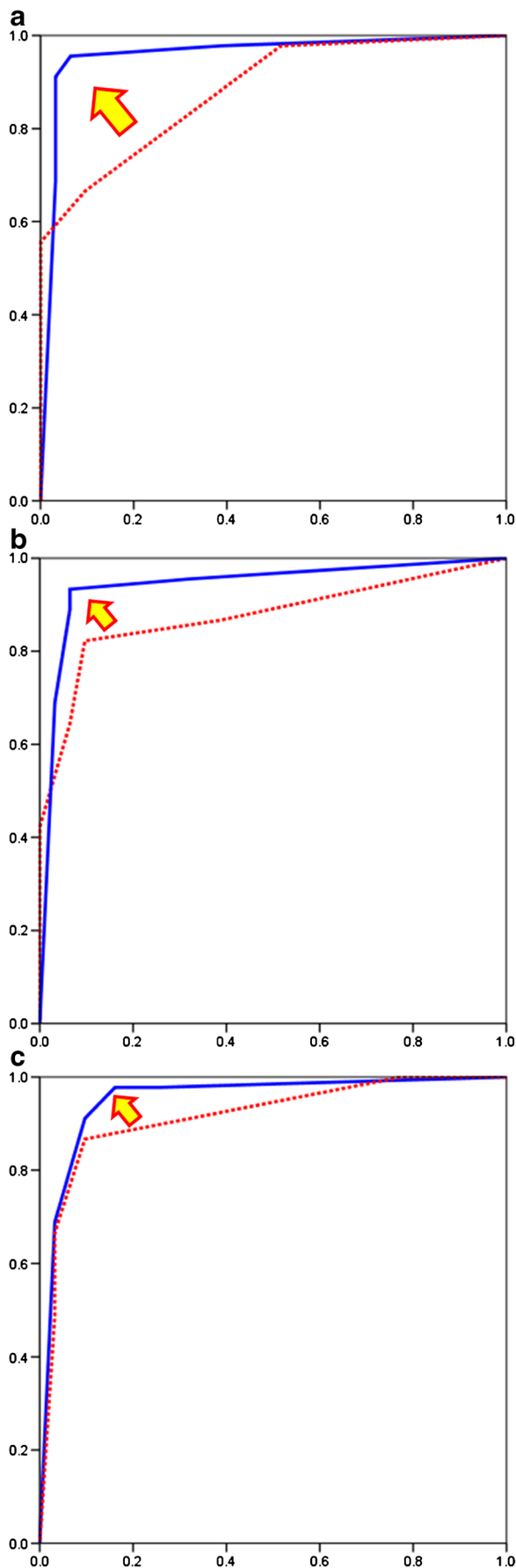
(PCI-iDose[4]). At the second session, the three radiologists were provided the optimized VMI (i.e., VMI_{40}) in addition to PCI-iDose[4]. Radiologists were asked to record the presence of active Crohn's disease for each patient using a 5-point confidence scale: 1, definitely absent; 2, probably absent; 3, possibly present; 4, probably present; and 5, definitely present. A confidence level ≥ 3 was considered to indicate a positive call of active Crohn's disease. The radiologists were informed the characteristic CTE findings of active Crohn's disease (i.e. mural hyperenhancement, mural thickening ≥ 3 cm, prominent vasa recta, fistula, or abscess). To minimize recall bias, two separate interpretation sessions were scheduled with a 2-week interval and the images were randomly presented.

Statistical analysis

Comparisons of quantitative parameters including CNR were performed using Kruskal-Wallis test with post-hoc test using pairwise comparisons between the subgroups according to Conover [19] to find the optimal VMI setting. Comparisons of qualitative parameters including contrast, noise, and overall image quality between PCI-iDose[4] and optimized VMI was performed using the Wilcoxon signed rank test. To assess the improvement in radiologists' performance in diagnosing active Crohn's disease, multi-reader, multi-case receiver operating characteristic (ROC) analysis was used [20, 21]. P values less than 0.05 were considered to indicate a significant difference. Statistical analyses were performed using commercial medical statistical packages (SPSS version 22, SPSS, IBM, Armonk, NY, USA; or MedCalc version 16, MedCalc Software, Mariakerke, Belgium) and a free software program (DBM-MRMC, version 2.2 software, http://perception.radiology.uiowa.edu).

Results

Radiation dose of dlDE-CTE

The average $CTDI_{vol}$ and DLP for dlDE-CTE including both enteric and portal phase images were 19.5 mGy (range, 14.8-

Fig. 4. A 28-year-old man with active Crohn's disease. **a** Conventional polychromatic image at 120 kVp reconstructed with iDose[4] (PCI-iDose[4]), **b** Virtual monoenergetic image at 70 keV (VMI_{70}), **c** Virtual monoenergetic image at 55 keV (VMI_{55}), and **d** Virtual monoenergetic image at 40 keV (VMI_{40}). Segmental enhancing bowel wall thickening (arrows) is well demonstrated at the terminal ileum suggesting active Crohn's disease. Note that lesion conspicuity is the best on VMI_{40} due to the high contrast of iodine. The degree of enhancement in the diseased bowel on PCI-iDose[4] is similar to that on VMI_{70} as the spectral centre of PCI at 120 kVp is approximately 70 keV. **e, f** Colonoscopic images show fold thickening with multiple aphthoid ulcers at the terminal ileum in (**e**) and deep ulceration and deformity in ileocecal valve in (**f**). Colonoscopic biopsy with clinical and imaging findings confirms the diagnosis of active Crohn's disease.
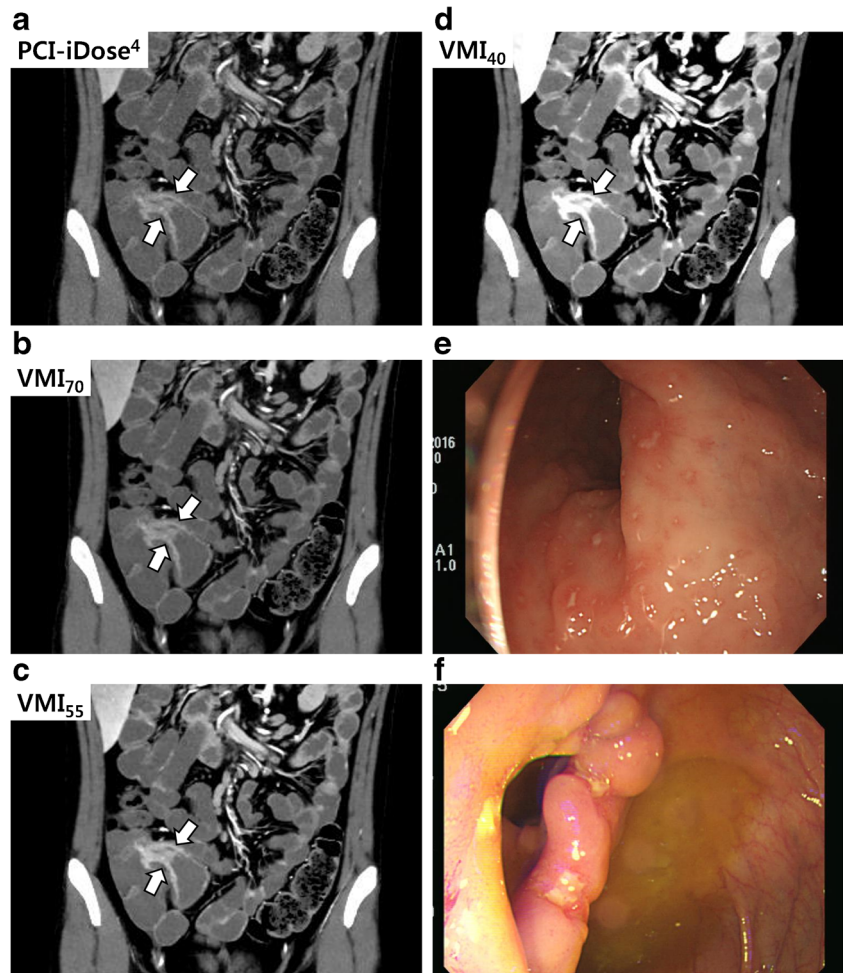
36.4 mGy) and 1043.7 mGy·cm (range, 741.2-2014.0 mGy·cm), respectively. Average effective dose was 15.7 mSv (range, 11.1-30.2 mSv).

Quantitative image analysis

CNR of each reconstructed image are presented in Fig. 2. Mean CNR ± standard deviation (SD) of the normal bowel wall (CNR_N) was significantly greatest on VMI_{40} (13.6 ± 6.5), followed by VMI_{55} (6.1 ± 3.2), VMI_{70} (2.0 ± 2.1), and PCI-iDose[4] (1.9 ± 1.6) ($P<0.001$). Post hoc tests according to Conover [19] revealed that all pairwise comparisons except CNR_N between VMI_{70} and PCI-iDose[4] were statistically significant ($P<0.05$). A similar trend was found for the abnormal bowel wall. CNR_{AB} was also greatest on VMI_{40} (9.4 ± 7.3), followed by VMI_{55} (6.5 ± 4.8), VMI_{70} (4.9 ± 3.1), and PCI-iDose[4] (3.7 ± 2.3) ($P<0.001$). On post hoc analysis according to Conover [19], all comparisons between reconstructed images were statistically significant ($P<0.05$).

The attenuation difference between the normal and abnormal bowel walls were greatest on VMI_{40} (93.4 ± 7.3), followed by VMI_{55} (50.6 ± 4.6), VMI_{70} (33.0 ± 2.7), and PCI-iDose[4]

(33.1 ± 2.9), which were significantly different by Kruskal-Wallis test ($P<0.001$). Post hoc tests revealed that all pairwise comparisons except the comparison between VMI_{70} and PCI-iDose[4] were statistically significant ($P<0.05$). Similar trend was found for % attenuation difference between normal and abnormal bowel walls. Value on VMI_{40} (70.5 ± 5.6) was higher than those on VMI_{55} (60.9 ± 4.7), VMI_{70} (54.2 ± 4.4), and PCI-iDose[4] (52.1 ± 4.7), albeit not statistically significant ($P=0.06$). For qualitative analysis, therefore, we determined VMI_{40} as an optimal VMI setting.

Qualitative analysis

Table 1 summarizes the comparative results of qualitative analysis between conventional PCI-iDose[4] and VMI_{40}. Mean image contrast on VMI_{40} (4.3 ± 0.6) was significantly better than that on PCI-iDose[4] (3.3 ± 0.6) ($P<0.001$) while mean noise on VMI_{40} (3.5 ± 0.6) was significantly higher than that on PCI-iDose[4] (4.0 ± 0.5) ($P<0.001$). Overall image quality of VMI_{40} (3.9 ± 0.7) was better than that of PCI-iDose[4] (3.8 ± 0.6); however, a statistical significance was marginal ($P=0.059$).

Fig. 5. A 24-year-old man with active Crohn's disease. **a** Conventional polychromatic image at 120 kVp reconstructed with iDose[4] (PCI-iDose[4]), **b** Virtual monoenergetic image at 70 keV (VMI$_{70}$), **c** Virtual monoenergetic image at 55 keV (VMI$_{55}$), and **d** Virtual monoenergetic image at 40 keV (VMI$_{40}$). Two segmental enhancing bowel wall thickenings (arrows) are well depicted at the distal ileum suggesting active Crohn's disease. Note that lesion conspicuity is best on VMI$_{40}$. The degree of enhancement in the diseased bowels on PCI-iDose[4] is similar to that on VMI$_{70}$ as the spectral centre of PCI at 120 kVp is approximately 70 keV. **e** Small bowel follow-through study obtained 7 years ago demonstrates the cobble-stone appearance (arrows) of the terminal ileum. At that time, the patient was diagnosed as having Crohn's disease by colonoscopic biopsy with clinical and imaging findings.
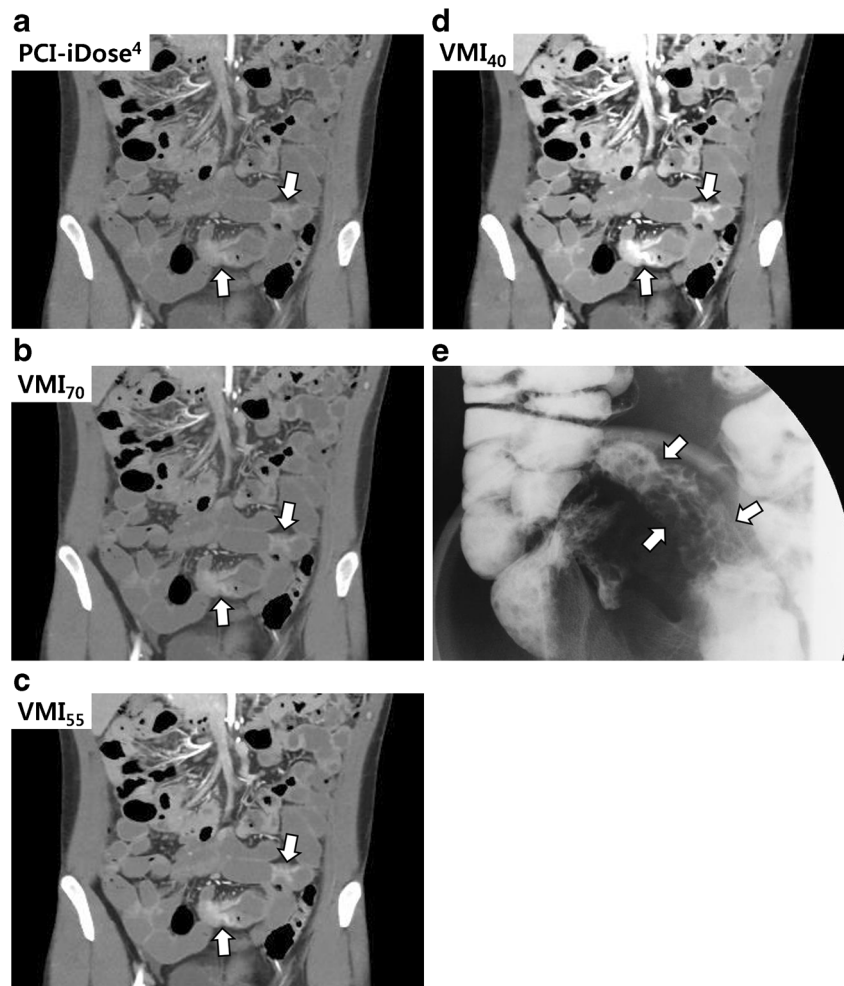
Radiologists' diagnostic performance for the diagnosis of active Crohn's disease

Tables 2 and 3 list the individual and overall performances of the three radiologists for the diagnosis of active Crohn's disease during the two successive independent review sessions. Corresponding ROC curves of the radiologists are shown in Fig. 3. When the most optimal VMI$_{40}$ images were added to PCI-iDose[4], overall area under the curve (AUC) of the three radiologists was significantly improved from 0.891 to 0.951 for the diagnosis of active Crohn's disease (P=0.009). Specifically, the AUC of all three radiologists was significantly improved from 0.882 to 0.959 for radiologist 1 (P=0.027), from 0.875 to 0.943 for radiologist 2 (P=0.027), and from 0.915 to 0.952 for radiologist 3 (P=0.035). The improvement was greater in the novice reader (0.077 for radiologist 1) than in the experienced readers (0.037 ~ 0.068 for radiologists 2 and 3).

When the most optimal VMI$_{40}$ images were added to PCI-iDose[4], sensitivity was significantly improved from 78.5% to 95.6% while specificity (90.3%) was not changed. Representative images are presented in Figs. 4, 5, and 6.

Discussion

Our study demonstrated that virtual monoenergetic images at 40 keV (VMI$_{40}$) provided the best CNR for both abnormal and normal small bowel walls on dual-layer DE-CTE. This may be because the enhanced contrast at 40 keV, being the closest keV to the iodine k-edge (33 keV) supersedes the increase in noise typically occurring in low keV images. Furthermore, in contrast to other image-based spectral algorithms, because the SDCT of our study uses a projection-based algorithm for noise reduction, the noise at low keV VMI might be more effectively suppressed. In addition, according to our study results, the CNRs for the normal bowel walls were not significantly different between VMI$_{70}$ and PCI-iDose[4], which may be explained by the fact that the spectral centre of a conventional PCI at 120 kVp is 65-70 keV [17].

Although no published studies are available evaluating lower keV images in Crohn's disease, there are several publications describing the usefulness of single-energy low kVp images [22; 23]. According to the previous reports, low-dose low kVp images reconstructed with iterative algorithm provide better CNR and comparable image quality with radiation

Fig. 6. A 25-year-old woman with active Crohn's disease. **a** Conventional polychromatic image at 120 kVp reconstructed with iDose^4 (PCI-iDose^4), **b** Virtual monoenergetic image at 70 keV (VMI$_{70}$), **c** Virtual monoenergetic image at 55 keV (VMI$_{55}$), and **d** Virtual monoenergetic image at 40 keV (VMI$_{40}$). A segmental enhancing bowel wall thickening (arrow) is well demonstrated at the sigmoid colon suggesting active Crohn's disease. Prominent vasa recta and fat creeping are also shown around the diseased bowel segment. Note that lesion conspicuity is the best on VMI$_{40}$. The degree of enhancement in the diseased bowel on PCI-iDose^4 is similar to that on VMI$_{70}$ as the spectral centre of PCI at 120 kVp is approximately 70 keV. **e** A colonoscopic image depicts an inflammatory stenosis with fold thickening at the sigmoid colon.
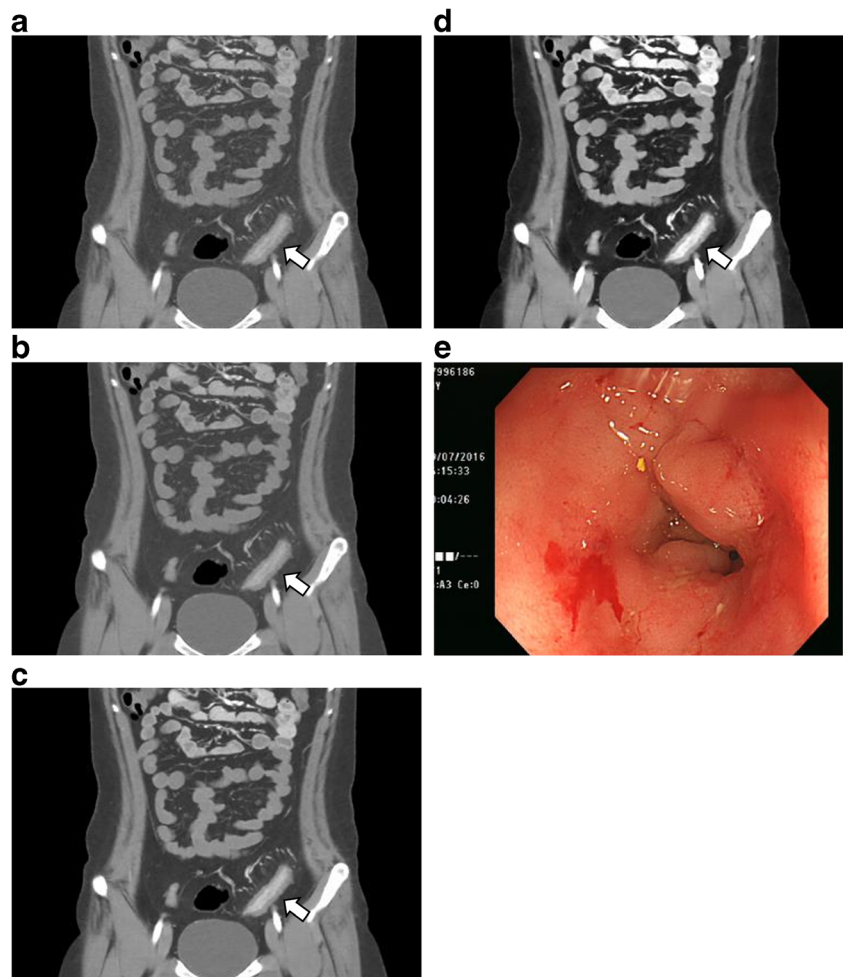
dose saving by 35-39% compared to standard-dose 120 kVp images reconstructed with filtered back projection algorithm [22, 23]. In terms of radiation dose, dlDE-CTE may not provide any benefit compared to low-dose low kVp images as radiation dose (15.7 mSv) of dlDE-CTE is higher than that (7.7 mSv) of low kVp single-energy CTE [22]. However, dlDE-CTE can provide a wide variety of spectral information such as iodine density map and Z_{eff} image, as well as VMI. Furthermore, if spectral separation technology in the detector improve in the future, we hope that the use of lower kVp such as 100 kVp dlDE-CTE could be possible, leading to further reduction of radiation dose.

Just as white light consists of an entire spectrum of colours, the X-ray photon beam produced by CT scanners consists of a spectrum of photons with a range of X-ray energies from low to high. The IQon spectral detector used in our study has the ability to simultaneously distinguish between X-ray photons of high and low energies with its unique dual-layer scintillator system. With this special design, every scan has spectral information, enabling the scanner to provide both conventional CT images, identical to regular CT, while providing additional spectral information as needed. For instance, virtual

monoenergetic (monochromatic) images provide images at energies of 40-200 keV in increments of 1 keV. In our study, we used CT images of 40 keV (VMI$_{40}$), 55 keV (VMI$_{55}$), and 70 keV (VMI$_{70}$) in addition to conventional 120 kVp polychromatic images (PCI-iDose^4).

In terms of subjective overall image quality, VMI$_{40}$ also showed better results than PCI-iDose^4. This may be partially because beam hardening artefacts which are characteristic of PCIs can be totally suppressed by VMIs. In addition, image degradation owing to other sources such as scatter and noise at low keV VMIs can be superseded by the high contrast at low keV.

We also found in our study that compared to conventional PCI-iDose^4 alone, radiologists' diagnostic performance for active Crohn's disease can be significantly improved with the addition of VMI$_{40}$. Of note, the improvement was shown to be greater in the novice radiologist than in the experienced radiologists. It may not be a surprising finding, however, as bowel wall thickening or mural enhancement in active Crohn's disease manifests subtly in its early stage, and thus, the detection of those findings may be troublesome in novice readers. Therefore, we believe that VMI$_{40}$ can aid radiologists

by showing brightly enhancing wall thickening more clearly through its high CNR. Even though there have been several reports in which DECT improved the conspicuity of decreased mural enhancement in small bowel ischemia [11, 17], there have been no publications regarding the optimization of keV levels and its diagnostic value for the detection of active Crohn's disease on dlDE-CTE. To the best of our knowledge, our study is the first article reporting the optimization of keV levels for small bowel depiction and describing the added diagnostic value in detecting active Crohn's disease using dlDE-CTE.

Another advantage of VMI on dlDE-CTE is that there is no need for upfront decision-making to obtain spectral information using DECT. Because of the ability of handling X-ray photons at the detector level, IQon spectral CT is the first and only CT machine built from the ground up for spectral imaging, so upfront decision-making was not necessary to obtain spectral information. Furthermore, retrospective on-demand spectral analysis of a region of interest can allow the physician to further investigate incidental findings without additional radiation exposure.

Finally, as expected, the CNR in VMIs is typically greater than in the corresponding conventional images and improves as VMI energy is reduced. However, with low energy monoenergetic images, 40 to 50 keV in particular, a higher low frequency noise component may result in a patchy appearance within the images. As very low keV images such as 40 keV are susceptible to the loss of low contrast features as well as the appearance of "non-real" features especially at low dose scans, the vendor recommends that CT images should be obtained at ≥ 120 kVp. In terms of spectral separation, however, the use of 140 kVp does have some advantages over 120 kVp due to the narrower spread of CT number for all body materials. However, as the use of 140 kVp inevitably increases radiation dose, we used 120 kVp for the dlDE-CTE used in our study.

Our study has several limitations. First, the number of patients in our study population was relatively small. Therefore, further studies using a larger sample size should be conducted to generalize our study results. Second, histologic confirmation was not done in all patients. However, considering that active Crohn's disease is occasionally diagnosed with a combination of clinical, endoscopic, laboratory, and imaging findings, we believe that this limitation may not be serious. In addition, we thoroughly investigated the clinical, endoscopic, and laboratory findings to confirm the patients' final diagnosis. Third, because we used a specific machine (IQon spectral CT) and iDose[4] for both PCI and VMI, our study cannot be generalized to other machines and other reconstruction algorithms such as filtered back projection or model-based iterative reconstruction. Thus, further comparative studies using different CT machines and reconstruction algorithms are warranted to investigate the advantages and disadvantages of each setting.

In conclusion, the lowest monoenergetic images (VMI$_{40}$) were demonstrated to provide the best CNR for abnormal and normal bowel walls on dlDE-CTE. In addition, radiologists' diagnostic performance for the diagnosis of active Crohn's disease was shown to be significantly improved with the addition of VMI$_{40}$ images to conventional PCI at 120 kVp.

Compliance with ethical standards

Guarantor The scientific guarantor of this publication is Se Hyung Kim.

Conflict of interest The authors of this manuscript declare no relationships with any companies, whose products or services may be related to the subject matter of the article.

Statistics and biometry No complex statistical methods were necessary for this paper.

Informed consent Written informed consent was waived by the Institutional Review Board.

Ethical approval Institutional Review Board approval was obtained.

Methodology
• retrospective
• observational
• performed at one institution

References

1. Ilangovan R, Burling D, George A, Gupta A, Marshall M, Taylor SA (2012) CT enterography: review of technique and practical tips. Br J Radiol 85:876–886

2. Raptopoulos V, Schwartz RK, McNicholas MM, Movson J, Pearlman J, Joffe N (1997) Multiplanar helical CT enterography in patients with Crohn's disease. AJR Am J Roentgenol 169:1545–1550

3. Boudiaf M, Jaff A, Soyer P, Bouhnik Y, Hamzi L, Rymer R (2004) Small-bowel diseases: prospective evaluation of multi-detector row helical CT enteroclysis in 107 consecutive patients. Radiology 233:338–344

4. Maglinte DD, Sandrasegaran K, Lappas JC, Chiorean M (2007) CT enteroclysis. Radiology 245:661–671

5. Fletcher JG (2009) CT enterography technique: theme and variations. Abdom Imaging 34:283–288

6. Elsayes KM, Al-Hawary MM, Jagdish J, Ganesh HS, Platt JF (2010) CT enterography: principles, trends, and interpretation of findings. Radiographics 30:1955–1970

7. Qiu Y, Mao R, Chen BL et al (2014) Systematic review with meta-analysis: magnetic resonance enterography vs. computed tomography enterography for evaluating disease activity in small bowel Crohn's disease. Aliment Pharmacol Ther 40:134–146

8. Greenup AJ, Bressler B, Rosenfeld G (2016) Medical imaging in small bowel Crohn's disease-computer tomography enterography, magnetic resonance enterography, and ultrasound: "which one is the best for what?". Inflamm Bowel Dis 22:1246–1261

9. Furukawa A, Saotome T, Yamasaki M et al (2004) Cross-sectional imaging in Crohn disease. Radiographics 24:689–702

10. Yeh BM, Shepherd JA, Wang ZJ, Teh HS, Hartman RP, Prevrhal S (2009) Dual-energy and low-kVp CT in the abdomen. AJR Am J Roentgenol 193:47–54

11. Darras KE, McLaughlin PD, Kang H et al (2016) Virtual monoenergetic reconstruction of contrast-enhanced dual energy CT at 70keV maximizes mural enhancement in acute small bowel obstruction. Eur J Radiol 85:950–956

12. Kaza RK, Platt JF, Al-Hawary MM, Wasnik A, Liu PS, Pandya A (2012) CT enterography at 80 kVp with adaptive statistical iterative reconstruction versus at 120 kVp with standard reconstruction: image quality, diagnostic adequacy, and dose reduction. AJR Am J Roentgenol 198:1084–1092

13. Morgan DE (2014) Dual-energy CT of the abdomen. Abdom Imaging 39:108–134

14. Huda W, Ogden KM, Khorasani MR (2008) Converting dose-length product to effective dose at CT. Radiology 248:995–1003

15. Bodily KD, Fletcher JG, Solem CA et al (2006) Crohn disease: mural attenuation and thickness at contrast-enhanced CT Enterography–correlation with endoscopic and histologic findings of inflammation. Radiology 238:505–516

16. Booya F, Fletcher JG, Huprich JE et al (2006) Active Crohn disease: CT findings and interobserver agreement for enteric phase CT enterography. Radiology 241:787–795

17. Potretzke TA, Brace CL, Lubner MG, Sampson LA, Willey BJ, Lee FT Jr (2015) Early small-bowel ischemia: dual-energy CT improves conspicuity compared with conventional CT in a swine model. Radiology 275:119–126

18. Ploussi A, Alexopoulou E, Economopoulos N et al (2014) Patient radiation exposure and image quality evaluation with the use of iDose4 iterative reconstruction algorithm in chest-abdomen-pelvis CT examinations. Radiat Prot Dosim 158:399–405

19. Conover WJ (1999) Practical nonparametric statistics, 3rd edn. Jonh Wiley & Sons, New York

20. Dorfman DD, Berbaum KS, Metz CE (1992) Receiver operating characteristic rating analysis. Generalization to the population of readers and patients with the jackknife method. Investig Radiol 27:723–731

21. Hillis SL, Berbaum KS, Metz CE (2008) Recent developments in the Dorfman-Berbaum-Metz procedure for multireader ROC study analysis. Acad Radiol 15:647–661

22. Kambadakone AR, Chaudhary NA, Desai GS, Nguyen DD, Kulkarni NM, Sahani DV (2011) Low-dose MDCT and CT enterography of patients with Crohn disease: feasibility of adaptive statistical iterative reconstruction. AJR Am J Roentgenol 196: W743–W752

23. Gandhi NS, Baker ME, Goenka AH, Bullen JA, Obuchowski NA, Remer EM et al (2016) Diagnostic accuracy of CT enterography for active inflammatory terminal ileal Crohn disease: comparison of full-dose and half-dose images reconstructed with FBP and half-dose images with SAFIRE. Radiology 280:436–445